Soil stoichiometric characteristics and influencing factors in karst forests at microtopography and microhabitat scales

Yi Dang[1,2,6], Hua Zhou[2,3], Wenjun Zhao[1,2], Yingchun Cui[1,2], Chengjiang Tan[4], Fangjun Ding[1,2], Yukun Wang[5], Run Liu[2], Peng Wu[1,2]

[1]Guizhou Libo Karst Forest Ecosystem Observation and Research Station, Guizhou Academy of Forestry, Guiyang, 550005, China
[2]Key Laboratory of National Forestry and Grassland Administration on Biodiversity Conservation in Karst Mountainous Areas of Southwestern China, Guizhou Academy of Forestry, Guiyang, 550005, China
[3]Guizhou Liping Rocky Desertification Ecosystem Observation and Research Station, Guizhou Academy of Forestry, Guiyang, 550005, China
[4]Maolan National Nature Reserve Administration, Libo, 558400, China
[5]School of Soil and Water Conservation, Beijing Forestry University, Beijing, 100083, China.
[6]Guizhou Leigongshan Forest Ecosystem Observation and Research Station, Guizhou Academy of Forestry, Guiyang, 550005, China

Correspondence: Run Liu (18285115229@163.com) and Peng Wu (zuishaoxu@163.com)

Abstract. To quantitatively assess soil stoichiometric characteristics in karst forests under complex microenvironments, this study systematically investigated the distribution patterns of soil nutrients and influencing factors across different microtopography and microhabitat scales in the Maolan karst forest. The results indicated that: (1) Soil nutrient contents exhibited strong spatial heterogeneity across the study area. (2) Microhabitat factors (stone gully, stone surface, soil surface) significantly influenced nutrient accumulation, although the response patterns varied among different nutrient elements. (3) Microtopographic factors (slope degree, slope aspect, slope position) were not only significantly correlated with soil nutrient patterns but also governed the spatial distribution gradients of certain nutrient elements. (4) Different response mechanisms of nutrients to microtopographic and microhabitat factors, combined with the different nutrient regulation and absorption strategies of various plant life forms (evergreen trees, deciduous trees, shrubs, herbs), collectively shaped the complex stoichiometric characteristics. The factors of microhabitat, microtopography, and plant life form exhibited synergistic effects on the soil stoichiometric characteristics in karst forests, with microhabitat and microtopographic factors playing a dominant role at this scale. Although biotic factors like plant life forms showed relatively weaker direct influences, their regulatory effects were closely interrelated with microhabitat and microtopographic factors. This multidimensional feedback mechanism reflects the complexity of nutrient cycling in karst soils.

Keywords. Karst; Microtopography; Microhabitat; Plant life form; Soil stoichiometry; Maolan National Nature Reserve

删除[dang]: To quantitatively evaluate the stoichiometric characteristics of karst forest soils and their response mechanisms to complex microenvironments, this study systematically investigated the patterns of soil nutrients and influencing factors across different microtopography and microhabitat scales in the Maolan karst forest.

删除[dang]: The variability of soil nutrient contents in the study area was generally moderate or higher, indicating strong spatial heterogeneity

设置格式[dang]: 字体: （默认）Times New Roman, （中文）Times New Roman, 10 磅, 字距调整: 0 磅, 英语(英国), （中文）德语(德国)

删除[dang]: Microhabitat factors (stone gully, stone surface, soil surface) significantly influenced nutrient accumulation, though different elements showed distinct response patterns to microhabitat variations

1 Introduction

Ecological stoichiometry, which integrates core theories from ecology, biology, chemistry, and other disciplines, is a science that studies the balance of energy and multiple chemical elements within biological systems. It focuses on how elemental balance regulates and influences ecological processes (e.g., growth, decomposition, and nutrient cycling), playing a crucial role in elucidating the coupling mechanisms between energy flow and elemental cycling in ecosystems (Chen et al., 2024). As a core component, soil stoichiometric characteristics serve not only as key indicators for assessing soil nutrient availability, microbial metabolic activity, and organic matter decomposition rates in fragile ecological regions but also as an important tool for understanding the coupling relationships of key soil nutrient elements in biogeochemical cycles and ecological processes (Joshi and Garkoti, 2023). Particularly in highly heterogeneous fragile ecosystems, the spatial variation of soil stoichiometric characteristics can act as a latent factor driving vegetation pattern succession (Chen et al., 2022). Previous studies have demonstrated that key environmental factors—including climate variables, geomorphic features, biotic components, and anthropogenic disturbances—primarily regulate the equilibrium states of major soil elements through biogeochemical pathways such as parent material weathering rates, litter accumulation patterns, and microbial decomposition processes. Analyzing soil stoichiometric characteristics enables not only effective inference of critical biogeochemical processes (e.g., organic matter decomposition status, microbial nutrient limitation conditions, and nutrient cycling efficiency) but also reveals mechanistic insights into how environmental drivers modulate process rates and directions by altering energy and nutrient availability. Therefore, analyzing soil stoichiometric characteristics and their driving mechanisms is a critical approach to understanding ecosystem functioning and vulnerability management (An et al., 2019). The related theoretical framework integrates the elemental allocation patterns across the soil-plant-microbe continuum into a unified dimension, providing a quantitative tool for understanding resource limitations and ecosystem stability (Sardans et al., 2021), and holds key significance for revealing environmental stress and ecological restoration potential in fragile ecological regions (Zhang et al., 2024).

China's karst region is renowned for its significant ecological fragility and habitat heterogeneity, covering a total area of approximately 1.3 million km², which accounts for 13.5% of the country's land area (Wu et al., 2025). As a typical karst ecosystem in southwest China, the Maolan karst region develops soils primarily from carbonate rocks, characterized by slow pedogenesis, thin and discontinuous soil layers, and severe shallow bedrock exposure (Tang et al., 2019). Driven by soil erosion, karstification, and hydrological processes, factors such as undulating microtopography, diverse karst microhabitats, and distinctive vegetation patterns collectively form highly heterogeneous surface microenvironment units. This heterogeneous combination shapes a patchy spatial differentiation pattern of soil moisture and nutrients in karst systems through modulating surface material redistribution pathways. Specifically, variations in moisture conditions, light availability, and material exchange efficiency across microenvironments often influence organic matter stabilization, litter decomposition rates, and microbial community structures, thereby profoundly reshaping the stoichiometric balance of soil

设置格式[dang]: 字体: （默认）Times New Roman, 10 磅, 字距调整: 0 磅

删除[dang]: '

删除[dang]: '

删除[dang]: The Maolan karst area, a typical karst ecosystem in southwestern China, features soils primarily derived from carbonate rocks. These soils are characterized by slow pedogenesis, shallow depth, and severe exposure of shallow bedrock

设置格式[dang]: 字体: （默认）Times New Roman, 10 磅, 非突出显示, 字距调整: 0 磅, 英语(英国)

设置格式[dang]: 字体: （默认）Times New Roman, 10 磅, 非突出显示, 字距调整: 0 磅, 英语(英国)

设置格式[dang]: 字体: （默认）Times New Roman, （中文）Times New Roman, 10 磅, 字距调整: 0 磅, 英语(英国), （中文）德语(德国)

major elements. Notably, in these fragmented karst landscapes, litter may be transported by wind or runoff, while plant roots may penetrate fractures to access water and nutrients. These processes likely render the stoichiometric relationships between plant and localized soil in karst slopes more complex than in non-karst ecosystems. Consequently, traditional nutrient cycling models based on homogeneity assumptions face significant limitations in such areas. Resource isolation driven by microenvironmental heterogeneity may not only intensify the decoupling of key nutrient cycling but also force plant-soil systems to adjust through stoichiometric homeostasis to adapt to localized resource constraints (Zhang et al., 2022). Previous studies have highlighted that at regional scales, climatic conditions and parent material are the dominant factors determining soil nutrient distribution patterns. However, at landscape and finer scales, the key drivers shaping soil stoichiometric characteristics are closely linked to non-zonal factors such as topographic features, microhabitat characteristics, and vegetation types. While extensive research has explored the stoichiometric characteristics of soil carbon (C), nitrogen (N), and phosphorus (P) at global or regional scales, the intrinsic mechanisms through which soil stoichiometric characteristics respond to the combined effects of microtopography, microhabitat, and surface vegetation in karst slope systems remain poorly understood (Feng et al., 2024). This knowledge gap limits our understanding of how soil and vegetation co-evolve in karst ecosystems. To address this gap, we examined soil-vegetation relationships across varied microhabitats and microtopographic positions in the Maolan karst area. By coupling systematic soil sampling with vegetation surveys of plant life forms, we characterized how soil stoichiometric properties vary with vegetation structure and topographic setting. Specifically, we address the following questions:

1) What are the spatial distribution patterns and heterogeneity of the major soil stoichiometric characteristics in the karst region?

2) What are the interrelationships among soil nutrient elements, and what is the intrinsic regulatory mechanism governing their stoichiometric balance?

3) How do factors such as microhabitat, microtopography, and plant life forms drive the formation of a patchy nutrient distribution pattern in karst forest soils?

This study will elucidate soil stoichiometric characteristics and their influencing factors in karst forests through multivariate analysis. The findings are expected to provide a new theoretical foundation for understanding the synergistic soil-vegetation adaptation mechanisms in karst ecosystems, while also offering a scientific underpinning for ecological restoration and sustainable management in the region.

2 Study area and methods

2.1 Study area

The study area is located within the Maolan National Nature Reserve in Guizhou Province, situated in the transitional slope zone from the Yunnan-Guizhou Plateau to the northern Guangxi hills. Its geographical coordinates range from 107°52’10”to

设置格式[dang]: 字体: （默认）Times New Roman, （中文）Times New Roman, 10 磅, 字距调整: 0 磅, 英语(英国), （中文）德语(德国)

设置格式[dang]: 字体: （默认）Times New Roman, （中文）Times New Roman, 10 磅, 字距调整: 0 磅, 英语(英国), （中文）德语(德国)

设置格式[dang]: 字体: （默认）Times New Roman, 10 磅, 字距调整: 0 磅, 英语(英国)

设置格式[dang]: 字体: （默认）Times New Roman, 10 磅, 字距调整: 0 磅, 英语(英国)

删除[dang]: Understanding of how soil stoichiometric characteristics respond to microtopography, microhabitats, and vegetation is still inadequate. This knowledge gap somewhat constrains our comprehension of the synergistic evolution mechanisms between soil and vegetation in karst ecosyste

删除[dang]: What are the relative contributions of microhabitat types, microtopographic features, and vegetation life forms to soil stoichiometric characteristics, and how do these factors interact with each other?

删除[dang]: Through a comprehensive multivariate analysis, this study aims to elucidate the underlying mechanisms shaping the stoichiometric characteristics of karst soils. The findings will provide a novel theoretical basis for understanding the coupled soil-vegetation adaptation

108°05’40”E and 25°09’20” to 25°20’50”N. The topography exhibits a distinct northwest-high, southeast-low pattern, with elevations ranging from 430.0 to 1078.6 m (predominantly 550-850 m) (Zhou et al., 2022). This region features a typical mid-subtropical monsoon humid climate, with meteorological data indicating: an annual average temperature of 15.3°C (coldest month: 5.2°C; warmest month: 23.5°C), annual precipitation of 1,752.5 mm (concentrated in summer), annual relative humidity of 83.0%, annual sunshine duration of 1,272.8 h, frost-free period of 315 d, and total annual solar radiation of 63.29 $kW \cdot m^{-2}$ (Wen and Jin, 2019).

The geological structure is predominantly composed of limestone and dolomite, forming a typical bare karst peak-cluster depression system with bedrock exposure exceeding 80.0%. Soil resources exhibit pronounced spatial constraints, primarily distributed in rock fissures with shallow and discontinuous profiles. Chemically, soils are characterized by high calcium content, base cation enrichment, and elevated organic matter, classified mainly as black limestone soils. The vegetation comprises primary karst evergreen-deciduous broadleaved mixed forests, representing azonal vegetation, with a forest coverage rate of 87.4%. This ecosystem stands as the best-preserved and most representative karst forest ecosystem at the same latitude in the Northern Hemisphere (Zhou et al., 2022).

2.2 Plot setting

As complete random sampling was impractical in the study area due to its status as a national nature reserve and the highly fragmented karst habitats, this study primarily employed a stratified random sampling method to establish sampling points. The specific procedure was as follows: based on a systematic investigation of existing fixed plots at the Libo Karst Forest Ecosystem Positioning Observation Research Station, a predefined stratification was conducted across five habitat strata: microhabitat, plant life form, slope degree, slope aspect, and slope position. Within each of these combination units (e.g., sharp slope + semi-shady slope + downslope + stone gully + evergreen trees), random grids were generated. After field reconnaissance to verify the feasibility of these points and eliminate unsuitable locations, alternative points were manually identified within the same stratum. Finally, the setup of all sampling points was completed. During the field investigation, geographic coordinates (latitude and longitude) and elevation data for each sample tree were recorded using high-precision handheld GPS devices. The slope aspect and slope degree of the plots were measured with professional compasses. Slope position and microhabitat information were determined through on-site observation (Figure 1). The number of plots corresponding to each classification stratum is detailed in the supplementary material (Table S1).

删除[dang]: 1

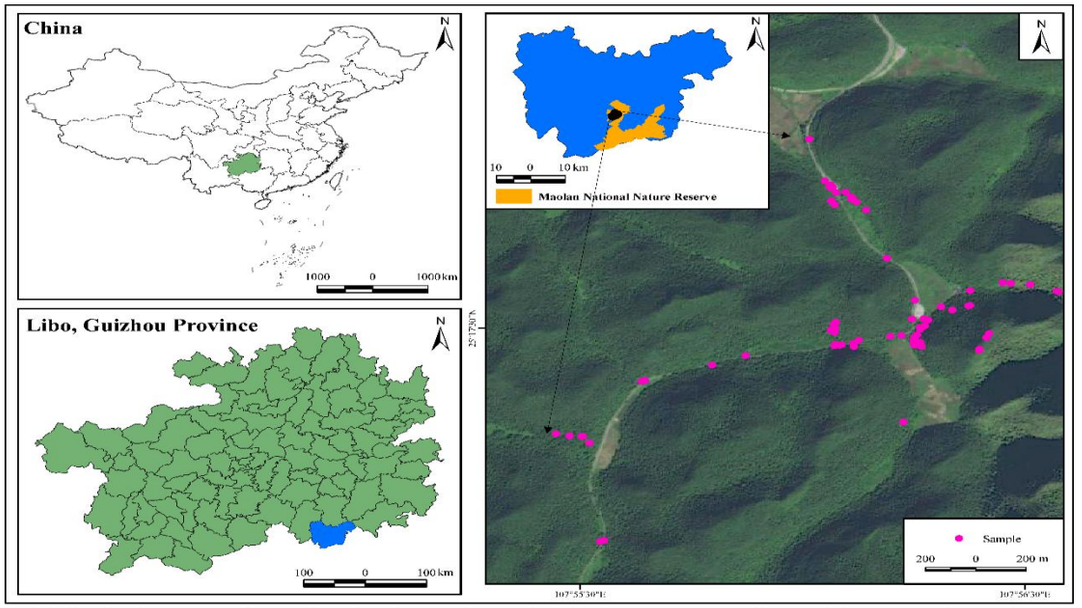

Figure 1. Spatial distribution maps of sampling sites in Maolan National Nature Reserve, Libo, Guizhou. Four-tier geolocation hierarchy: China's national framework (top-left) with green area indicating Guizhou Province; Libo County boundaries (bottom-left) with blue zone marking study townships; Maolan National Nature Reserve (top-right) with orange area delineating protected core zone; Satellite imagery of sampling sites (bottom-right) with pink circles designating soil sampling locations. (Scale bars: 1000 km/100 km/10 km/200 m; north arrows: N).

2.3 Microtopography division

The microtopographic features of the study area can be systematically classified according to the following scheme (Wu et al., 2025):

Slope position: upslope, midslope, downslope, and depression (four classes);

Slope degree: flat slope (≤ 5°), gentle slope (5 - 15°), tilted slope (15 - 25°), steep slope (25 - 35°), and sharp slope (≥ 35°) (five classes);

Slope aspect: shady slope (337.5-22.5°, 22.5-67.5°), semi-shady slope (67.5-112.5°, 292.5-337.5°), flat land, semi-sunny slope (112.5-157.5°, 247.5-292.5°), and sunny slope (157.5-247.5°) (five classes).

2.4 Microhabitat division

Microhabitat refers to the micro-scale environmental units where individual organisms or populations reside, characterized by local topography, substrate type, and microclimate. While no universally accepted definition exists regarding its spatial scale, this study adopts a karst forest microhabitat classification system established in prior research. Practically, microhabitats in the study area were categorized into three types—stone surface, stone gully, and soil surface—based on

principles of representativeness, distinctiveness, and operational feasibility (Wu et al., 2025). The specific classification criteria are as follows (Table 1 and Figure S1):

Table 1. Classification criteria for various types of microhabitats.

Microhabitat types	Bedrock exposure rate	Gully depth	Surface soil cover area
Stone surface microhabitat	>50%	≤30 cm	≤1 m²
Stone gully microhabitat	>50%	>30 cm	≤1 m²
Soil surface microhabitat	≤50%	≤30 cm	>1 m²

2.5 Soil sample collection and determination

Due to the typical karst terrain of the study area, characterized by an extremely thin surface soil layer, samplers completed soil collection using only a shovel and cutting rings (100 cm^3), without requiring tools like soil augers designed for deep soil sampling. Upon reaching a sampling point, the area within a 20 cm radius of plant root distribution was selected. After removing surface litter, three intact soil cores were collected using cutting rings. Following the manual removal of non-soil materials, the samples were thoroughly mixed, ensuring a net weight of ≥ 500 g per sample. The samples were immediately coded, sealed in sterile sampling bags, and temporarily stored in a portable cooler for subsequent analysis.

Samples were processed in batches upon returning to the laboratory. For the determination of pH, hydrolyzable nitrogen (HN), available phosphorus (AP), available potassium (AK), exchangeable calcium (ExCa), and exchangeable magnesium (ExMg), the soil samples were passed through a 2-mm nylon sieve. This procedure preserved the intact soil structure, avoided the destruction of active components through grinding, and ensured that the extraction of readily available nutrients reflected true field conditions. For the determination of soil organic carbon (SOC), total nitrogen (TN), total phosphorus (TP), total potassium (TK), total calcium (TCa), and total magnesium (TMg), the soil samples were passed through a 0.149-mm sieve. All residual material not passing the 0.149 mm sieve was subjected to secondary grinding using an agate mortar until it completely passed through the sieve. This portion was then thoroughly mixed with the sieved fine soil fraction to form an analytical sample representing the entirety of the original soil matrix (after removal of > 2 mm gravel). This approach ensures thorough sample homogenization, eliminating interference from particle size effects on total elemental analysis and guaranteeing the completeness of digestion/fusion. Furthermore, it allows for the inclusion of elements from all soil components in the analysis, preventing deviation of measurement results from true values due to the discarding of any fraction, thereby ensuring the accuracy and representativeness of the data. All analyses were strictly performed using air-dried soil samples. During sample processing, this study ensured the timeliness and consistency of the air-drying process, and soil samples were stored under cool and dry conditions to minimize potential alterations during air-drying. Preprocessing and analytical conditions were standardized across all samples to ensure data comparability and reliability (Specific analytical methods and core instruments are detailed in Table S2) (Yang and Da, 2006).

删除[dang]:
设置格式[dang]: 字体:（默认）Times New Roman,
设置格式[dang]: 题注
设置格式[dang]: 字体:（默认）Times New Roman,
带格式表格[dang]
设置格式[dang]: 字体:（默认）Times New Roman,
设置格式[dang]: 字体:（默认）Times New Roman,
设置格式[dang]: 字体: 六号
设置格式[dang]: 字体:（默认）Times New Roman, 六
设置格式[dang]: 字体: 六号
设置格式[dang]: 字体: 六号
设置格式[dang]: 字体: 六号
删除[dang]: The stone surface microhabitat refers to
删除[dang]: (Table 1)
删除[dang]:
设置格式[dang]: 字体:（默认）Times New Roman,
删除[dang]: Soil sample preparation strictly adhered to th
删除[dang]:

2.6 Vegetation survey and plant nutrient analysis

During soil sample collection, field personnel simultaneously recorded the plant species and life forms at each sampling point and collected representative leaf samples. Plant species were identified to the species level using taxonomic methods, and their Latin names were documented. Plant life forms were classified into four categories—evergreen trees, deciduous trees, shrubs, and herbs—based on standard botanical criteria and adapted to the local conditions of the study area. Leaf sampling followed the principle of representativeness: using high-pruners, well-developed branches from the east, south, west, north, upper, middle, and lower parts of the canopy were clipped. Fully expanded, disease-free, intact leaves without petioles were then picked from these branches. The collected leaves were thoroughly mixed, and a subsample of 30–50 leaves was retained using the quartering method. These samples were labeled, sealed in zip-lock bags, and stored in a portable refrigerator for subsequent analysis (Specific analytical methods and core instruments are detailed in Table S3). All soil and plant nutrient analyses in this study were conducted in strict accordance with the relevant *Chinese Forestry Industry Standards (LY/T 1210-1275-1999)* (Yang and Da, 2006).

2.7 Data processing and analysis

This study used mass contents to characterize soil nutrient indicators (SOC, TN, TP, etc., totaling 12 items; see supplementary material Table S4 for details). The stoichiometric ratios of the elements were calculated as mass ratios (SOC:TN, SOC:TP, SOC:TK, etc., totaling 9 items; see supplementary material Table S5 for details). Data analysis was performed using SPSS 25.0 and Excel 2016 for statistical processing, and graphical outputs were generated via Origin 2021. The Kolmogorov-Smirnov (K-S) test was applied to assess data normality. Prior to correlation analysis, raw data were logarithmically transformed [ln(x+1)] to meet ANOVA assumptions and normality requirements. Homogeneity of variance was tested before conducting ANOVA, with LSD or Tamhane's T2 methods selected for multiple comparisons based on test outcomes (Nagamatsu et al., 2003). For associations between soil stoichiometric characteristics (continuous variables) and numerically coded environmental factors (ordinal variables), this study employed Spearman's rank correlation for determination. The coefficient of variation is denoted as CV in this study, and the criteria for classifying its variation intensity are as follows: weak ($CV \leq 0.20$), moderate ($0.20 < CV < 0.50$), and strong ($CV \geq 0.50$) (Han et al., 2019).

This study employed redundancy analysis (RDA) using CANOCO 5.0 software to examine the relationships between soil stoichiometric characteristics and environmental factors. Environmental variables were coded as follows: slope positions (upslope, midslope, downslope, depression) were assigned values 1-4; slope degrees (flat, gentle, tilted, steep, sharp) were assigned 1-5; slope aspects (shady, semi-shady, flat land, semi-sunny, sunny) were assigned 1-5; microhabitats (soil surface, stone gully, stone surface) were assigned 1-3; and life forms (evergreen trees, deciduous trees, shrubs, herbs) were assigned 1-4. Monte Carlo permutation tests were applied to assess the significance of the constrained ordination model and to quantify the influence of individual environmental factors on soil stoichiometric characteristics. Variance partitioning analysis (VPA) was performed using the vegan package in R 4.4.1 to determine the explanatory contributions of different

设置格式[dang]: 字体: 倾斜

设置格式[dang]: 字体: 倾斜

删除[dang]:
The preparation of plant samples referred to the industry standard LY/T 1267–1999. Carbon (C) content was determined by the potassium dichromate oxidation–external heating method; nitrogen (N) content by the Kjeldahl meth

删除[dang]:
Table 3. Analytical methods and core instrumentation for determining plant properties.
Detection Indicator
Standard Method

删除[dang]: 2

删除[dang]: 3

删除[dang]: '

categories of environmental factors and their interactions. The influencing factors included three groups: (i) microenvironmental factors (slope degree, slope aspect, slope position, microhabitat), (ii) plant structural factors (plant species, life forms), and (iii) plant nutrient factors (plant nutrient contents: C, N, P, K, Ca, Mg). Soil stoichiometric characteristics served as response variables, encompassing all 11 soil nutrient contents and 9 stoichiometric ratios. The adjusted R^2 value was used to evaluate the goodness-of-fit of the model.

3 Results and Analysis

3.1 Stoichiometric characteristics of soil in the Maolan Karst region

Soil nutrient contents in the study area generally exhibited strong spatial variability. Kolmogorov-Smirnov (K-S) tests indicated that only total phosphorus (TP) and total potassium (TK) followed a normal distribution ($P > 0.05$), while the majority of other nutrients deviated from normality. Analysis based on the coefficient of variation (CV) revealed high variability for most nutrients, particularly for available phosphorus (AP) (CV = 0.95). In contrast, only TP, TK, and total magnesium (TMg) showed moderate variability (CV ≤ 0.50). The spatial patterns suggested that the maximum values of soil pH and nutrient contents were frequently associated with stone surfaces and downslope positions, whereas the minimum values were often found on soil surface microhabitats and midslope positions. (Detailed descriptive statistics are provided in supplementary material Tables S4 and S5).

3.1.1 Soil stoichiometric characteristics across different slope degrees

Soil nutrients and their stoichiometric ratios exhibited distinct distribution trends across different slope degrees. Statistical analysis (Tables S6 and S7) revealed that the mean values of most nutrient contents were highest on flat slopes and lowest on sharp and steep slopes, with significant differences observed between the maximum and minimum values for certain elements. For example, the difference in TP between flat slopes and sharp slopes was highly significant (MD = 0.222, 95% CI [0.058, 0.385], $P = 0.009$). Only a few elements, such as TMg, displayed an opposite trend, with the highest enrichment observed on sharp slopes. The highest mean stoichiometric ratios were almost all concentrated on sharp and steep slopes, while the lowest means were mainly scattered across slope types other than flat slopes, with a relatively high frequency on tilted slopes. However, the distribution trend of TCa:TMg differed from the others, being highest on flat slopes and lowest on gentle slopes. Although the former was 1.54-fold higher than the latter, the difference was not significant (MD = 0.234, 95% CI [-0.119, 0.587], $P = 0.19$) (Figure 2).

删除[dang]: . These patterns preliminarily highlight the significant influence of microtopography and microhabitat on nutrient spatial distribution.

删除[dang]: 2

删除[dang]: 3

删除[dang]: Table S4

删除[dang]: 2

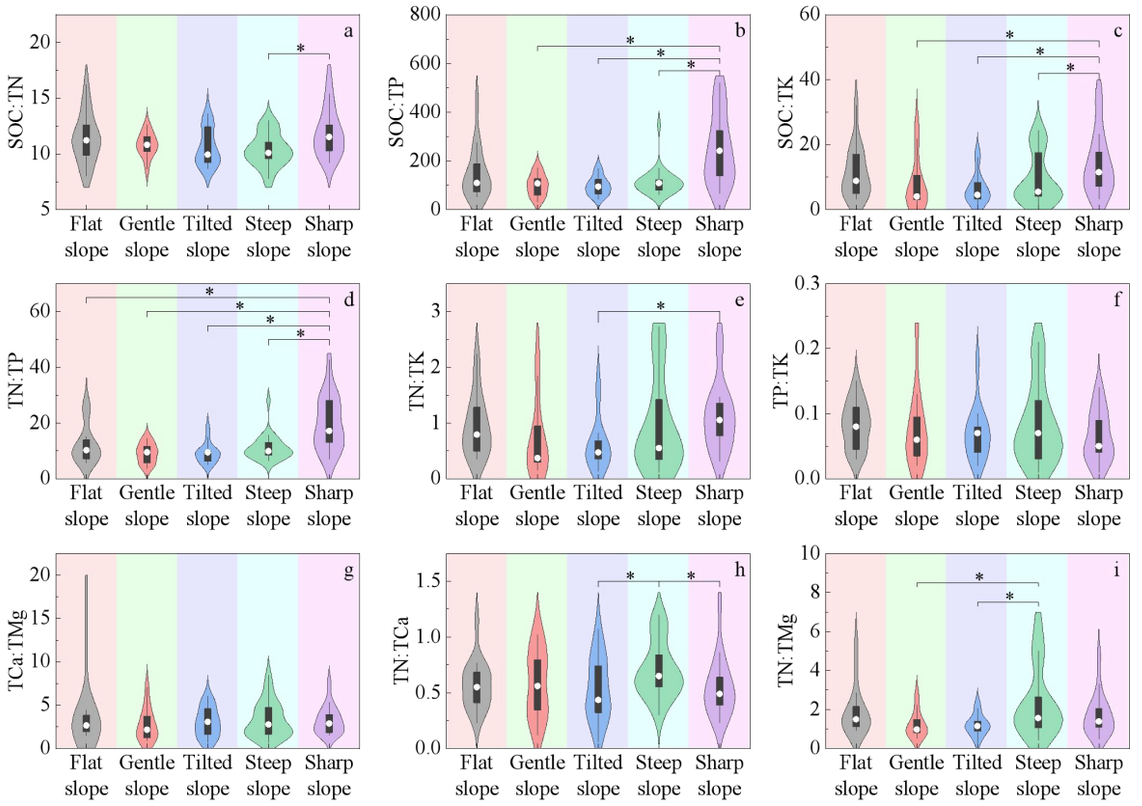

Figure 2. Distribution differences in stoichiometric ratios of major soil nutrients across different slope degree types, presented as violin plots overlaid with box plots. The Y-axis of each subplot denotes the values of corresponding ratios, while the X-axis represents slope degree types. An asterisk (*) indicates significant intergroup differences ($P < 0.05$), with black horizontal lines connecting groups exhibiting differences. The number of samples (n) for each slope degree type is as follows: flat slope (n = 16), gentle slope (n = 12), tilted slope (n = 14), steep slope (n = 27), sharp slope (n = 17).

3.1.2 Soil stoichiometric characteristics across different slope aspects

Major soil nutrients were highest on flat land, followed by shady slopes, and lowest on sunny slopes. Statistical analysis (Tables S8 and S9) showed that the minimum mean values of most elements were predominantly concentrated on sunny slopes and semi-sunny slopes, while the maximum mean values occurred more frequently on flat land, shady slopes, or semi-shady slopes. The differences between these extremes were often significant. For example, the difference in SOC between semi-shady slopes and sunny slopes was highly significant (MD = 0.501, 95% CI [0.141, 0.860], $P = 0.007$). However, the distribution trends of a very few elements were exceptional; for example, TK content was highest on sunny slopes, but the differences among all slope aspects were not significant. Due to the uneven distribution of elemental contents across slope aspects, the minimum mean values of stoichiometric ratios were mainly found on sunny slopes and similar areas, while the maximum means were scattered without a clear trend. In general, most elemental stoichiometric ratios were relatively similar

删除[dang]: Table S5

across different slope aspects. Only a few, such as SOC:TK, reached significant differences between aspects like semi-shady slopes and sunny slopes (MD = 0.462, 95% CI [0.054, 0.870], P = 0.027) (Figure 3).

删除[dang]: 3

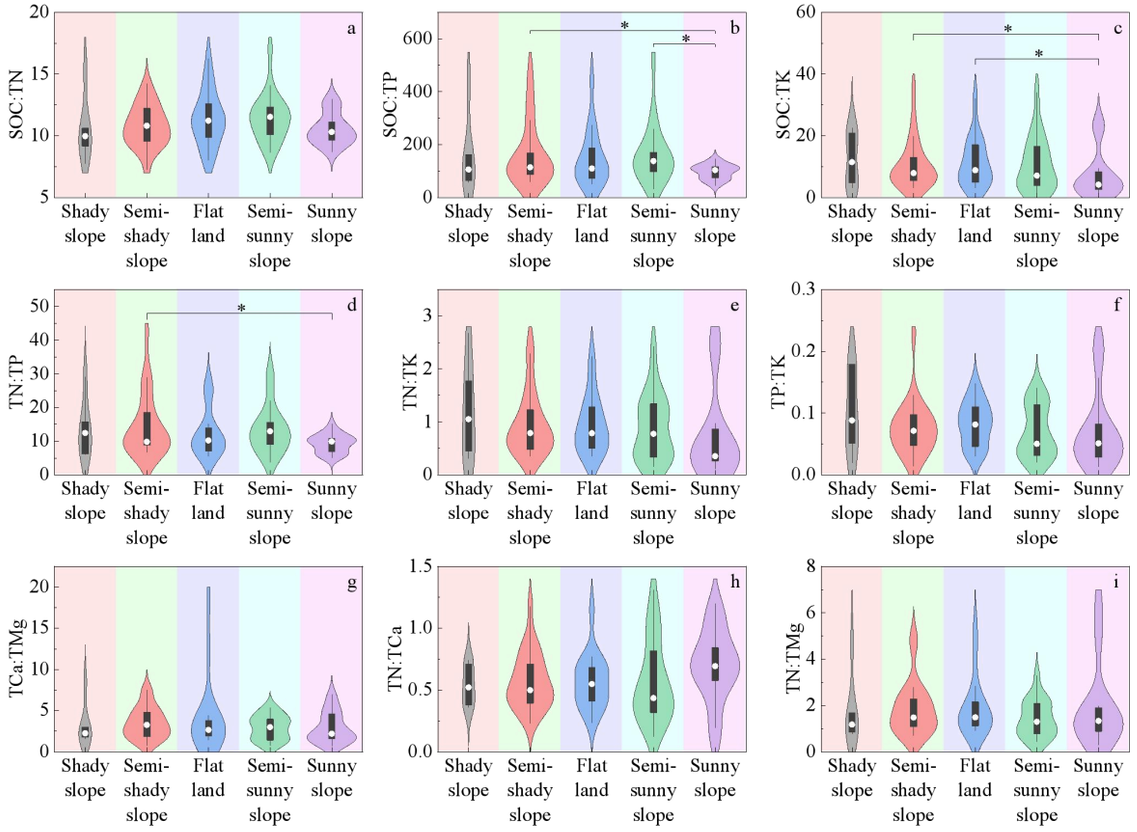

Figure 3. Distribution differences in stoichiometric ratios of major soil nutrients across different slope aspect types, presented as violin plots overlaid with box plots. The Y-axis of each subplot denotes the values of corresponding ratios, while the X-axis represents slope aspect types. An asterisk (*) indicates significant intergroup differences (P < 0.05), with black horizontal lines connecting groups exhibiting differences. The number of samples (n) for each slope aspect type is as follows: shady slope (n = 6), semi-shady slope (n = 22), flat land (n = 16), semi-sunny slope (n = 19), sunny slope (n = 23).

3.1.3 Soil stoichiometric characteristics across different slope positions

Soil primary nutrients and their stoichiometric ratios exhibited distinct distribution patterns across different slope positions. Statistical analysis (Tables S10 and S11) showed that the mean content of most nutrients was highest at the upslope position and lowest at the midslope position, with significant differences often observed between these two positions. For example, the difference in TN between the upslope and midslope positions was highly significant (MD = 0.735, 95% CI [0.294, 1.176], P = 0.001). Due to the relatively higher contents of SOC and TN at the upslope position, the maximum values of their related stoichiometric ratios (e.g., SOC:TN, TN:TP) were also primarily distributed at the upslope position. Constrained by the distribution of element contents across slope positions, the various stoichiometric ratios were relatively similar between the

删除[dang]: Table S6

downslope position and depression, with almost no significant differences observed. In contrast, significant differences existed for nearly all ratios between the midslope and downslope positions, except for TN:TCa. Among these, the mean difference in SOC:TN between the midslope and downslope positions was even highly significant (MD = 0.112, 95% CI [0.038, 0.186], $P = 0.004$) (Figure 4).

删除[dang]: 4

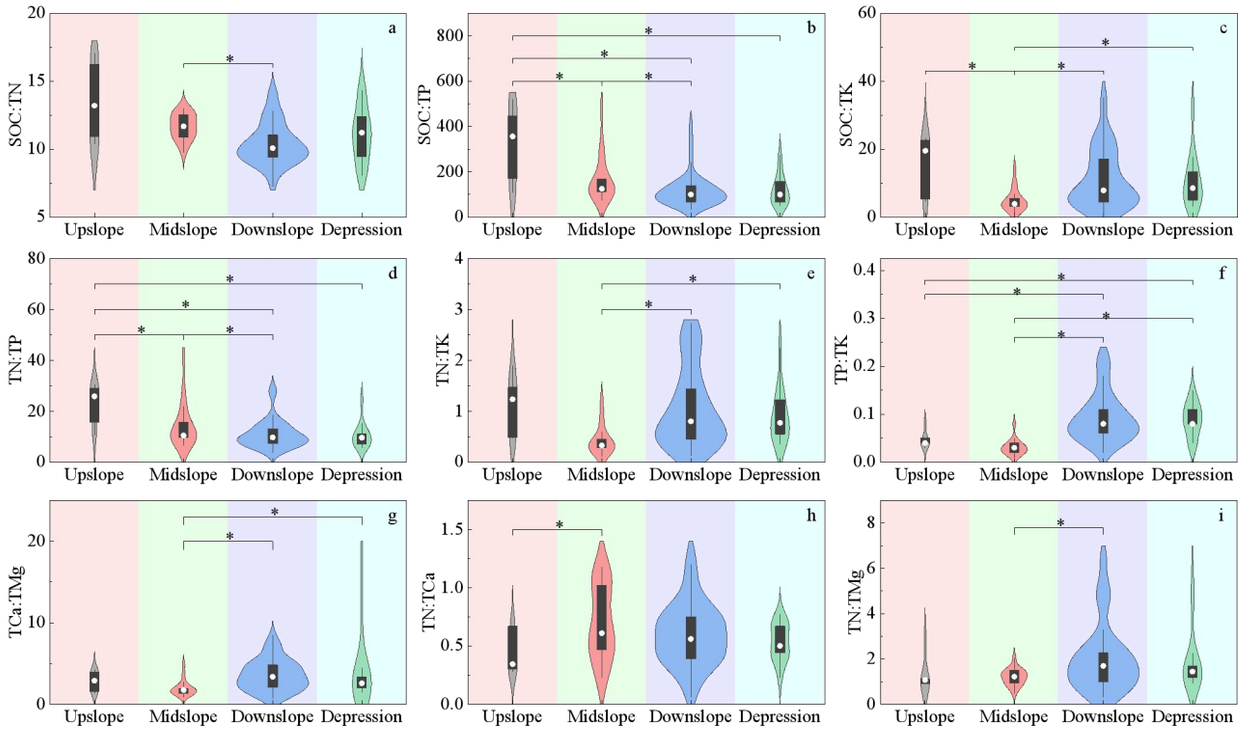

Figure 4. Distribution differences in stoichiometric ratios of major soil nutrients across different slope position types, presented as violin plots overlaid with box plots. The Y-axis of each subplot denotes the values of corresponding ratios, while the X-axis represents slope position types. An asterisk (*) indicates significant intergroup differences ($P < 0.05$), with black horizontal lines connecting groups exhibiting differences. The number of samples (n) for each slope position type is as follows: upslope (n = 6), midslope (n = 18), downslope (n = 49), depression (n = 13).

3.1.4 Soil stoichiometric characteristics across different microhabitats

The distribution of major soil nutrients across the three microhabitats generally followed similar trends: both elemental contents and stoichiometric ratios tended to be lower on the soil surface and higher on the stone surface, with significant differences often observed between these two microhabitats. Values in the stone gully generally fell between the other two. Statistical analysis (Tables S12 and S13) indicated that carbon and nitrogen were more enriched in the stone surface microhabitat compared to other elements. Consequently, the maximum mean values of major nutrient stoichiometric ratios (e.g., SOC:TP, SOC:TK, TN:TP, TN:TK) were significantly greater in the stone surface microhabitat than in the soil surface

删除[dang]: Table S7

microhabitat. However, influenced by the distribution pattern of TCa, the trend for TN:TCa was opposite to the general pattern, with its mean value highest in the soil surface microhabitat and lowest in the stone surface microhabitat. The value in the soil surface microhabitat was 1.29 times that in the stone surface microhabitat, and the difference was significant (MD = 0.091, 95% CI [0.006, 0.177], $P = 0.004$) (Figure 5).

删除[dang]: 5

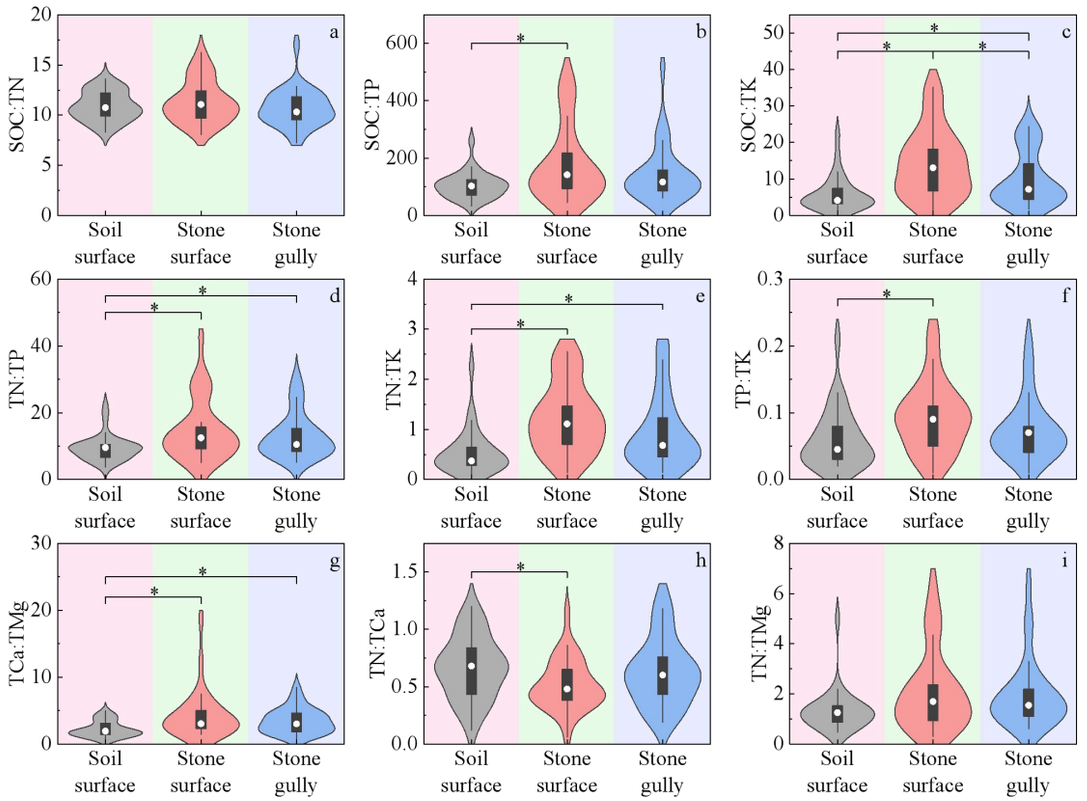

Figure 5. Distribution differences in stoichiometric ratios of major soil nutrients across different microhabitats, presented as violin plots overlaid with box plots. The Y-axis of each subplot denotes the values of corresponding ratios, while the X-axis represents microhabitats. An asterisk (*) indicates significant intergroup differences ($P < 0.05$), with black horizontal lines connecting groups exhibiting differences. The number of samples (n) for each microhabitat type is as follows: soil surface (n = 28), stone gully (n = 29), stone surface (n = 29).

3.1.5 Soil stoichiometric characteristics across different life forms

The distribution trends of most nutrients were similar in the rhizosphere soils of the four plant life forms. Statistical analysis (Tables S14 and S15) indicated that the mean values of element contents and stoichiometric ratios were generally highest in herb soils and lowest in evergreen or deciduous tree soils, with the differences often being significant. Among these, the difference in TP between herb and evergreen tree soils was even highly significant (MD = 0.214, 95% CI [0.063, 0.365], $P = 0.006$). However, the distribution pattern of some elements, such as TK, was opposite to that of most elements, showing

删除[dang]: Table S8

significantly higher values in trees than in shrubs and herbs. This regular distribution of element contents resulted in corresponding patterns for the major nutrient stoichiometric ratios. Higher values were mostly concentrated in the herb life form, while lower values occurred more frequently in deciduous tree soils. For example, the stoichiometric ratios TN:TK and TP:TK were influenced not only by the aforementioned distribution trend of TK but also by the fact that elements like TN and TP were present in greater, or significantly greater, quantities in herb soils compared to deciduous tree soils (Figure 6).

删除[dang]: 6

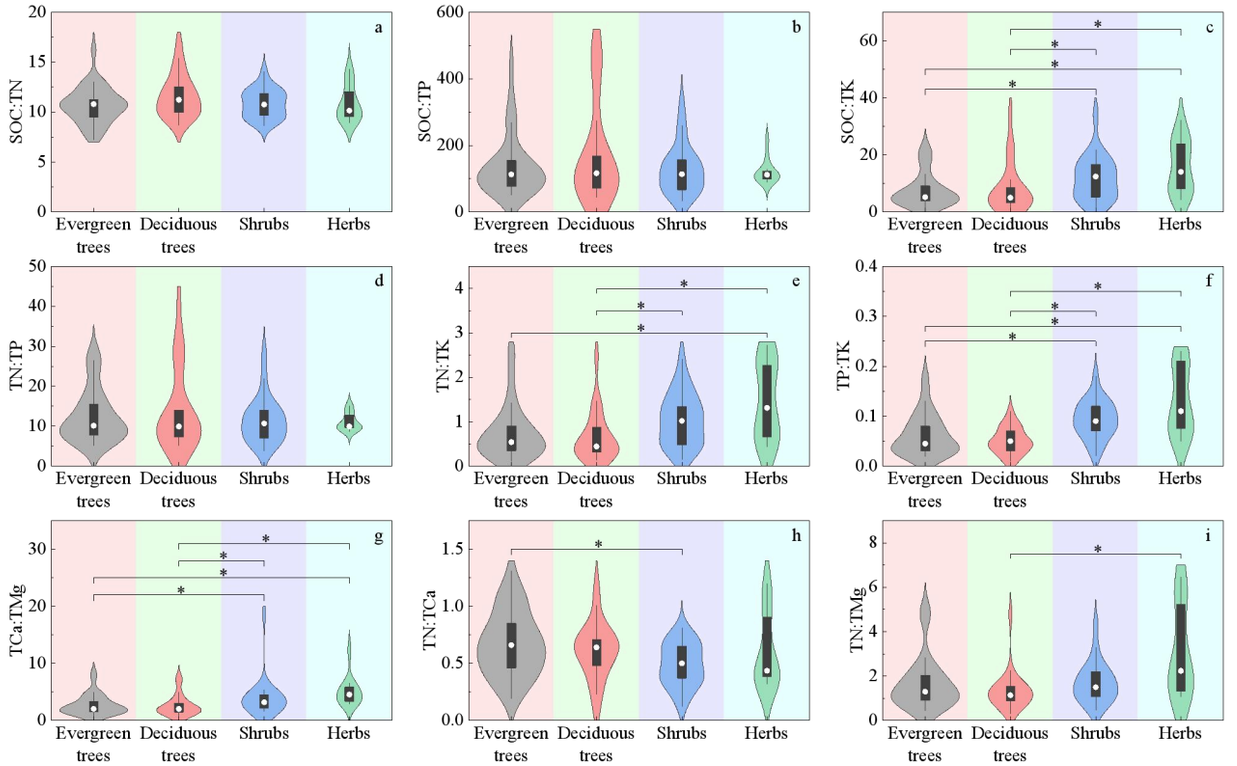

Figure 6. Distribution differences in stoichiometric ratios of major soil nutrients within the rhizosphere zones of different plant life forms, presented as violin plots overlaid with box plots. The Y-axis of each subplot denotes the values of corresponding ratios, while the X-axis represents plant life forms. An asterisk (*) indicates significant intergroup differences ($P < 0.05$), with black horizontal lines connecting groups exhibiting differences. The number of samples (n) for each plant life form is as follows: evergreen trees (n = 32), deciduous trees (n = 21), shrubs (n = 21), herbs (n = 12).

3.2 Correlation analysis between soil nutrient contents and stoichiometric ratios in karst regions

The correlation matrix revealed complex interrelationships among soil nutrients and their stoichiometric characteristics (Figure S2). Soil SOC and TN contents exhibited a strong co-variation trend (r = 0.94, $P < 0.01$), and both showed significant positive correlations with most other nutrients (e.g., HN, TCa, and ExCa). In contrast, TK content was significantly negatively correlated with SOC, TN, and several key stoichiometric ratios (e.g., SOC:TP, TN:TMg). Available phosphorus (AP) demonstrated a more independent pattern, showing significant positive correlations only with TCa and

删除[dang]: 1

SOC. Close associations were also observed among different stoichiometric ratios; for instance, SOC:TK and TN:TK exhibited a highly significant positive correlation (r = 0.95, $P < 0.01$). These association patterns indicate tightly coupled relationships among major nutrient elements such as carbon, nitrogen, and calcium, as well as the unique distribution pattern of certain individual elements within the karst soil system.

3.3 Influencing factors of soil stoichiometric characteristics in karst regions

To investigate the effects of factors including microtopography, microhabitat, and plant life forms on soil stoichiometric characteristics, this study performed Redundancy Analysis (RDA) and correlation analysis. The results indicated that the first two RDA axes cumulatively explained 23.1% of the relationship between the soil stoichiometric variables and the environmental factors (microtopography, microhabitat, plant life forms). Monte Carlo permutation tests revealed that microhabitat was the most significant factor influencing the soil stoichiometric characteristics ($P < 0.01$), uniquely explaining 10.4% of the variance. It was followed by slope position (8.0%), plant life forms (5.3%), and slope aspect (1.8%). In contrast, the effect of slope degree was not statistically significant ($P = 0.15$), exhibiting the lowest explanation rate (1.4%) and contribution rate (5.6%) (Table 2). Spearman's rank correlation analysis (Table S16) further supported the RDA results: 90% of the soil stoichiometric indicators showed significant or highly significant correlations with microhabitat, whereas the proportion of indicators significantly correlated with other factors ranged from 30% to 70%. The RDA biplot (Figure 7) clearly illustrated that microhabitat was positively correlated with most soil nutrient contents and their stoichiometric ratios (e.g., TCa, TN, SOC:TK) and was negatively correlated with only a few indicators (e.g., TK, TN:TCa).

删除[dang]:

删除[dang]: The underlying driving mechanisms will be thoroughly analyzed in the Discussion section.

删除[dang]: ; Figure 7

设置格式[dang]: 字体: （默认）Times New Roman, 10 磅

删除[dang]: (Table S9)

删除[dang]: 3

设置格式[dang]: 字体: （默认）Times New Roman, 10 磅

删除[dang]: '

删除[dang]: 9

删除[dang]: 7

设置格式[dang]: 字体: （默认）Times New Roman, 10 磅

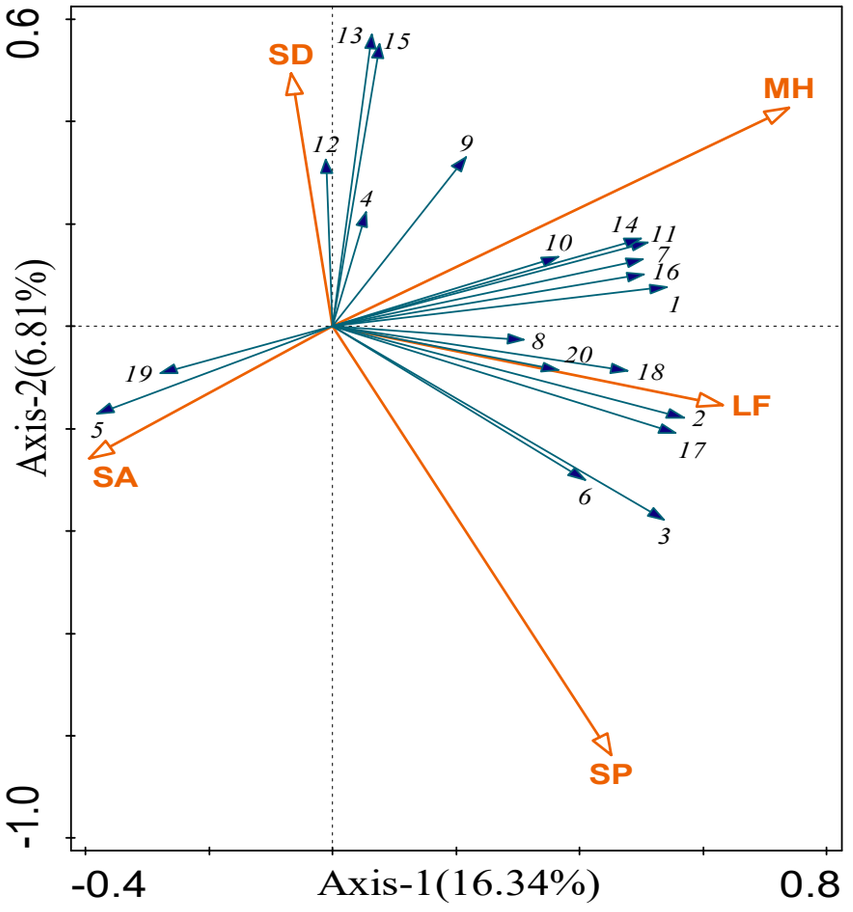

Figure 7. Ordination biplot of redundancy analysis (RDA) for soil stoichiometric characteristics and environmental factors. Axes: RDA1 (16.3% variance explained) and RDA2 (6.8% variance explained). Blue arrows represent stoichiometric variables: 1(TN), 2(HN), 3(TP), 4(AP), 5(TK), 6(AK), 7(TCa), 8(ExCa), 9(TMg), 10(ExMg), 11(SOC), 12(SOC:TN), 13(SOC:TP), 14(SOC:TK), 15(TN:TP), 16(TN:TK), 17(TP:TK), 18(TCa:TMg), 19(TN:TCa), 20(TN:TMg). Red arrows represent environmental variables: MH (Microhabitat), SP (Slope Position), SA (Slope Aspect), SD (Slope Degree), LF (Life Form). Arrow length denotes variable contribution; inter-arrow angles reflect correlations. Origin (0,0) serves as the reference point.

Table 2. Results of Monte Carlo test of effects of environmental factors on Soil stoichiometric characteristics.

Environmental factor	Explains rate/%	Contribution rate/%	*F* value	*P* value
Microhabitat	10.4	40.7	10.8	<0.01
Slope position	8.0	27.1	7.8	<0.01
Life forms	5.3	18.8	5.7	<0.01
Slope aspect	1.8	7.9	2.4	<0.05
Slope degree	1.4	5.6	1.7	>0.01

To comprehensively quantify the contributions of different factor categories to soil stoichiometric characteristics, this study performed variance partitioning analysis (VPA; Figure 8) using three groups of predictors: microenvironmental factors (slope degree, slope aspect, slope position, and microhabitat), plant structural factors (plant species and life forms), and plant nutrient factors (plant nutrient contents). Collectively, these factors explained 34.2% of the total variance in the soil stoichiometric dataset. Among them, microenvironmental factors exhibited the highest unique contribution (23.5%), while plant structural factors and plant nutrient factors showed considerably lower individual contributions (only 2.5% and 1.0%, respectively). Statistical analysis incorporating geomorphic features and plant distribution patterns indicated that the contents of various plant nutrients showed moderate to strong coefficients of variation (CV) and differed significantly among life forms (Fig. S3). Furthermore, even for the same plant species, the combinations of microhabitat and microtopography in which it survives can vary considerably. Therefore, plant nutrient content is not an intrinsic property independent of the environment but is profoundly influenced by the specific microenvironment (e.g., microhabitat type, microtopography type) in which the plant grows. Notably, among the interaction effects, the joint explanatory proportions of microenvironmental factors – plant nutrient factors (3.8%) and microenvironmental factors – plant structural factors (2.1%), although relatively modest, were both higher than that of plant structural factors–plant nutrient factors (1.1%).

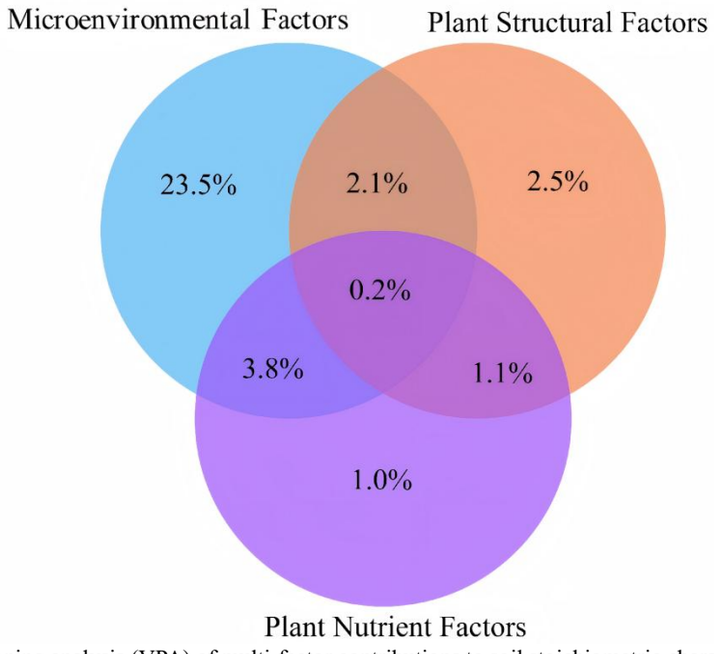

Figure 8. Variance partitioning analysis (VPA) of multi-factor contributions to soil stoichiometric characteristics. Tri-color overlapping system denotes environmental factor contributions: Blue: Microenvironmental factors (slope/aspect/position/microhabitat); Orange: Plant structural factors (species/life form); Purple: Plant nutrient factors (C/N/P/K/Ca/Mg contents); Values in overlapping areas indicate joint explanatory effects. Residuals = 65.8%.

删除[dang]: 8

设置格式[dang]: 字体: （默认）Times New Roman, 10 磅, 字距调整: 0 磅, 英语(英国)

设置格式[dang]: 字体: （默认）Times New Roman, 10 磅, 字距调整: 0 磅

删除[dang]: Regarding interaction effects, the joint contributions of microenvironmental with plant nutrient factors (3.8%) and of microenvironmental with plant structural factors (2.1%) were both higher than that between the two plant-related factor groups (1.1%). Overall, the three-way interaction among all factor categories was minimal, explaining merely 0.2% of the variance.

4 Discussion

4.1 Stoichiometry-based nutrient cycling strategies in karst forest soils

This study reveals exceptionally high rates of soil organic matter decomposition and nitrogen mineralization in the Maolan karst region, demonstrating that the ecosystem sustains nitrogen supply through rapid nutrient turnover. This strategy is substantiated by elevated mean concentrations of SOC and TN (125.08 and 11.20 $g \cdot kg^{-1}$, respectively) and a low SOC:TN ratio (10.83). Building on prior research from Turkish karst systems—which established that microbial activity intensifies when SOC:TN < 20, potentially driving decomposition rates beyond organic matter accumulation—we deduce that the study area employs a "high-speed carbon-nitrogen cycling" strategy (Dindaroglu et al., 2021). This adaptation likely arises from accelerated microbially decomposition and nitrogen mineralization, enabling survival in fragmented habitats with shallow soils. Furthermore, the low coefficient of variation (CV) in SOC:TN ratios suggests synchronized responses of SOC and TN release/migration to environmental conditions. When microbes degrade organic carbon skeletons and release nitrogen, fixed stoichiometric ratios emerge, corroborating findings from other studies that soil SOC:TN ratios remain relatively stable (Li et al., 2017).

Unlike nitrogen, phosphorus limitation in the study area is primarily driven by microtopography-mediated nutrient redistribution processes. Although the mean TP concentration (0.99 $g \cdot kg^{-1}$) exceeds the regional average, elevated SOC:TP (326.58) and TN:TP (22.91) ratios in upslope positions indicate that microorganisms and plants in these microtopographies likely face severe phosphorus scarcity. In fact, phosphorus limitation is not uncommon in karst regions, with similar findings frequently reported in studies of other karst forests worldwide (e.g., karst forests in Puerto Rico) (Medina et al., 2017). This pattern may stem from phosphorus' limited adsorption capacity in soils, making it prone to loss through raindrop splash and surface runoff erosion. We suggest that excessively high SOC:TP and TN:TP ratios could trigger microbial competition for limited phosphorus during decomposition, reducing nutrient use efficiency in karst soils. In response to strong phosphorus limitation, vegetation in upslope areas of karst regions often adopts a conservative, defensive growth strategy, enhancing carbon accumulation capacity to improve stress resistance. The nutrient return from decomposing fine roots and leaves further contributes to elevated SOC:TP and TN:TP ratios in these soils.

Furthermore, this study identified calcium as a central hub in coupling biogeochemical processes in karst soils. This is evidenced by the synergistic variation between the soil calcium-magnesium balance and the contents of major nutrients. For instance, soils under shrub and herb vegetation exhibited simultaneous enrichment in TCa:TMg ratios alongside elevated SOC, TN, and TP contents. Similarly, stone surface microhabitats displayed higher levels of both TCa and SOC. These cross-factor associations converge on a unified mechanism: calcium forms organic-inorganic complexes that enhance soil organic matter stability, modulate microbial community structure and abundance, and facilitate microaggregate formation (Pastore et al., 2022). This mechanism effectively links vegetation litter input, microbial activity, and long-term soil nutrient

设置格式[dang]: 字体:（默认）Times New Roman, 10

删除[dang]:

retention, creating a positive feedback loop. Thus, calcium transcends its role as a mere nutrient element and functions as a key chemical bridge connecting nutrient cycling and retention (Yang et al., 2023).

Although TMg concentrations did not differ significantly among plant life forms, herb soils exhibited higher or significantly higher TN:TMg ratios compared to other life forms. We attribute this pattern to the prevalence of herbs in depression microtopographies. Previous studies indicate that runoff convergence in such terrain accelerates carbonate rock dissolution, releasing nitrogen while promoting magnesium loss, thereby creating a negative correlation between soil nitrogen and magnesium (Perakis et al., 2013). Consequently, the elevated TN:TMg ratios in herb soils may reflect the combined effects of specific microtopographic features and associated biogeochemical processes.

4.2 Main driving factors of soil nutrient patterns in karst forests

This study reveals that the spatial heterogeneity of soil nutrients in the Maolan karst forest is not randomly distributed but rather forms an ordered pattern jointly shaped by key environmental factors such as microhabitat, microtopography, and plant life form. The combined regulation of these multiple factors on the input, migration, accumulation, and loss of soil nutrients constitutes a crucial driving mechanism for soil nutrient cycling in karst forests.

4.2.1 Microhabitat factors

This study identifies microhabitats as a dominant driver of spatial nutrient differentiation in karst soils, primarily through modulating rock exposure rates and material exchange intensity at the soil-rock interface, thereby redistributing water and nutrients. Most nutrients in the study area exhibit a “stone surface enrichment–soil surface depletion” pattern, likely linked to nutrient heterogeneity and poor connectivity in karst systems. Stone surface microhabitats with high rock exposure create semi-closed or partially enclosed microenvironments due to exposed bedrock barriers, which retain surface water and accumulate litter, ultimately converting it into humus. In contrast, soil surface microhabitats lack rock barriers and exhibit continuous soil layers, leading to nutrient loss via intensive leaching. Previous studies highlight that spatial heterogeneity in rock exposure regulates hydrological connectivity and divergence patterns in material transport pathways, acting as a critical environmental factor shaping biogeochemical cycling of soil nutrients. Under the combined effects of rock dissolution and soil erosion, the land surface becomes fragmented, impeding nutrient transport and contributing to the relative stability of soil stoichiometric characteristics within microhabitats (Waring et al., 2020). Similar patterns occur in other subtropical karst regions, where stone surface microhabitats show higher organic matter accumulation, macroaggregate content, and superior soil aggregate stability and nutrient retention compared to soil surfaces microhabitats (Bi et al., 2024). This improved soil nutrient condition may further regulate surface vegetation community structure, root growth, and litter dynamics, thereby enhancing soil nutrient inputs and ultimately establishing a positive feedback loop.

设置格式[dang]: 字体: （默认）Times New Roman, 10 磅, 字距调整: 0 磅

设置格式[dang]: 字体: （默认）Times New Roman, 10 磅, 字距调整: 0 磅, 英语(英国)

设置格式[dang]: 字体: （默认）Times New Roman, 10 磅, 字距调整: 0 磅

设置格式[dang]: 字体: （默认）Times New Roman, 10 磅, 字距调整: 0 磅

删除[dang]: (Peng and Dai, 2022)

设置格式[dang]: 字体: （默认）Times New Roman, 10 磅, 字距调整: 0 磅, 英语(英国)

设置格式[dang]: 字体: （默认）Times New Roman, 10 磅, 字距调整: 0 磅

设置格式[dang]: 字体: （默认）Times New Roman, 10 磅, 字距调整: 0 磅

设置格式[dang]: 字体: （默认）Times New Roman, 10 磅, 字距调整: 0 磅

设置格式[dang]: 字体: （默认）Times New Roman, 10 磅, 字距调整: 0 磅

设置格式[dang]: 字体: （默认）Times New Roman, 10 磅, 字距调整: 0 磅

设置格式[dang]: 字体: （默认）Times New Roman, 10 磅, 字距调整: 0 磅

4.2.2 Microtopographic factors

This study reveals that microtopographic factors significantly influence the spatial distribution patterns of multiple soil elements, with enrichment zones of certain elements often coinciding with flat slopes, shady slopes, and upslope positions. Slope degree primarily regulates nutrient retention and loss through gravitational effects, where steeper gradients exacerbate runoff and erosion, leading to poorer nutrient conditions. Consequently, soil nutrient input-output dynamics may vary significantly across slope gradients, a phenomenon previously observed in karst regions such as Bodoquena in Brazil (Silva et al., 2017). However, some elements display contrasting patterns—for instance, AP concentrations are lower in flat and gentle slopes compared to steep and sharp slopes. This inversion may arise from frequent waterlogging in gentler terrains, which increases free calcium carbonate content in soils. The subsequent formation of calcium phosphate salts reduces phosphorus bioavailability for vegetation. Similar patterns have been documented in the Yucatan karst region of Mexico (Campo, 2016).

The influence of slope aspect primarily stems from heterogeneous solar radiation distribution. This study observed that nutrient depletion zones were concentrated on sunny and semi-sunny slopes, rarely occurring on other slope aspects. This pattern may arise from relatively abundant habitat resources on shady slopes, where reduced evaporation rates enhance soil resistance to erosion, preserving nutrients and creating superior ecological niches for vegetation. In contrast, sunny slopes with intense solar radiation and drier soils may restrict litter decomposition, limiting nutrient release. Similar findings have been reported in studies of the Caspian Sea karst region (Smirnova and Gennadiev, 2017). Non-karst studies in the Qinghai-Tibet Plateau also documented comparable nutrient patterns, attributing them to habitat heterogeneity enabling shady slope vegetation and microbial communities to develop superior functional traits, thereby improving soil nutrient replenishment and retention (Zhang et al., 2022). Therefore, this study concludes that although cloud cover and vegetation modulate solar radiation, slope aspect remains a dominant driver of spatial radiation differentiation in karst regions. This radiation heterogeneity generates significant spatial gradients in heat and moisture distribution across slopes, profoundly influencing soil moisture-nutrient coupling processes.

In the Maolan karst region, this study reveals that certain elements (e.g., SOC, TN, TCa, and TMg) exhibit significantly higher concentrations at upslope positions compared to midslope positions. This differentiation in soil stoichiometric characteristics among slope positions may arise from erosion disparities and variations in vegetation growth strategies. Conventional studies outside karst regions suggest that runoff migrating along slopes typically transports water and nutrients from upslope to downslope or depression areas, resulting in thinner soils and reduced water/nutrient retention capacity at upslope positions (Yu et al., 2020). However, in karst systems, high rock exposure, fragmented terrain, and unpredictable infiltration patterns lead to distinct element migration and accumulation dynamics compared to non-karst slopes. Researchers in China's Guangxi karst regions observed higher nutrient levels at upslope positions compared to midslope and downslope

设置格式[dang]: 字体: （默认）Times New Roman, 10

areas, attributing this pattern to unique erosion processes and vegetation's role in mediating soil nutrient dynamics on karst slopes (Dou et al., 2024).

4.2.3 Plant life form factors

This study reveals that plant life forms regulate soil stoichiometric characteristics through differential nutrient uptake and return strategies, resulting in systematic enrichment patterns of multiple nutrients in rhizosphere soils of different life forms. This phenomenon may arise from vegetation actively adapting to surface environments while simultaneously modulating soil stoichiometric dynamics via root activity and litter nutrient return. Variations in litter decomposition could generate structural heterogeneity in forest floor nutrient cycling, a finding corroborated in studies of eastern Mediterranean karst ecosystems (Babur et al., 2022). In our research, significant differences in near-surface litter accumulation were observed among plant life forms in karst mountainous regions, where shrubs and herbs, with clustered growth habits, intercept more litter not only from their own senescence but also from arboreal litter transported by wind or slope runoff, whereas trees retain less litter due to minimal basal branching compared to the dense ground-level accumulation in shrub/herb communities. For example, some researchers have observed that the understory vegetation layer can extensively intercept and regulate the spatial distribution pattern of litter, with litter accumulation decreasing with increasing distance from the base of shrub and herb vegetation (M. Dearden and A. Wardle, 2008). Other researchers suggest that the interception of litter by the understory vegetation layer may alter its microenvironment (including light, moisture, soil, and microbial communities), thereby influencing the decomposition trajectory of the litter (He et al., 2013). Therefore, the relationship between vegetation type and soil stoichiometric characteristics is not invariant. Numerous factors—including plant species, growth stage, community composition, rock obstruction, and runoff scour—may exert direct or indirect effects on karst soil stoichiometry, contributing to the complexity of plant-mediated influences on soils in karst mountainous regions.

4.3 Specificity of karst forest soils and research limitations

In summary, this study reveals that the soil stoichiometric characteristics of the Maolan karst forest are shaped by complex interactions among microhabitat, microtopography, and plant life forms, resulting in a highly heterogeneous "patchy" distribution pattern. The essence of this pattern lies in the inherent characteristics of karst ecosystems: soil thinness, high rock exposure rates, and fragmented topography. These underlying conditions profoundly alter and amplify the spatial heterogeneity of ecological processes. For instance, the strong segmentation effect of the bedrock not only exacerbates the local enrichment and loss of nutrients by influencing hydrological connectivity, but the intense weathering and dissolution processes of the bedrock release calcium ions that significantly influence regional nutrient cycling. This makes calcium a key element connecting the rock-soil-vegetation system, a process rarely encountered in non-karst regions.

设置格式[dang]: 字体: （默认）Times New Roman, 10 磅, 字距调整: 0 磅

设置格式[dang]: 字体: （默认）Times New Roman, 10 磅, 字距调整: 0 磅

设置格式[dang]: 字体: （默认）Times New Roman, 10 磅, 字距调整: 0 磅

设置格式[dang]: 字体: （默认）Times New Roman, 10 磅, 字距调整: 0 磅

设置格式[dang]: 字体: （默认）Times New Roman, 10 磅, 字距调整: 0 磅

设置格式[dang]: 字体: （默认）Times New Roman, 10 磅, 字距调整: 0 磅

设置格式[dang]: 字体: （默认）Times New Roman, 10 磅, 字距调整: 0 磅

设置格式[dang]: 字体: （默认）Times New Roman, 10 磅, 字距调整: 0 磅

删除[dang]:

It should be noted that the sampling strategy of this study was based on predefined discrete habitat stratifications. While this approach enhanced sampling feasibility within the complex karst terrain, such discretization may not fully capture continuous environmental gradients, thereby constituting an inherent limitation in characterizing microenvironmental heterogeneity and sampling design in such habitats. Therefore, future research should transcend this static stratification framework and commit to adopting continuous environmental gradient monitoring and high-resolution sampling strategies to overcome this limitation. This will better capture the complexity of karst ecosystems and facilitate a paradigm shift from discrete stratification to process-driven approaches.

5 Conclusions

This study, based on systematic surveys of soils in the Maolan karst forest, reveals the spatial patterns of soil stoichiometric characteristics and identifies their primary driving factors. Results demonstrate that soil nutrients exhibit high spatial heterogeneity at the microenvironmental scale, a pattern closely linked to divergent elemental cycling strategies. Soil carbon and nitrogen cycling show strong synchrony, whereas phosphorus distribution is predominantly governed by microtopography-driven nutrient redistribution processes. As a critical linkage in biogeochemical processes, calcium-magnesium balance dynamics are tightly associated with microhabitat and plant life form factors. Notably, the spatial heterogeneity of soil nutrients in the Maolan karst forest is not randomly distributed but forms a “patchy” pattern shaped by key environmental drivers—microhabitat, microtopography, and plant life forms. Among these, microhabitat exerts the strongest influence on soil stoichiometric characteristics, directly governing the ‘enrichment in stone surface microhabitats and depletion in soil surface microhabitats’ pattern. Microtopography not only correlates significantly with nutrient patterns but also drives gradient distribution trends for certain elements. Although the influence of plant life forms is relatively weaker, their regulatory effects are often closely linked to microenvironmental factors such as microhabitat and microtopography. This multi-factor synergistic regulation profoundly influences the input, transport, accumulation, and loss of soil nutrients, serving as a key driving mechanism of nutrient cycling in karst forest soils. Collectively, these findings enhance understanding of the co-adaptation mechanisms between soils and vegetation in fragile karst ecosystems and provide critical theoretical foundations for precise ecological restoration and management strategies in karst regions.

设置格式[dang]: 字体: （默认）Times New Roman, 10 磅, 字距调整: 0 磅, 英语(英国)

Data availability. The data generated in this study are available from the first or corresponding author upon reasonable request.

Author contributions. Methodology, Data curation, Writing - review & editing, Writing - original draft, Visualization, Validation: YD. Investigation, Supervision: HZ. Formal analysis, Supervision: WZ. Investigation, Validation: YC. Conceptualization, Formal analysis: CT. Formal analysis, Investigation: FD. Formal analysis, Investigation: YW. Methodology, Supervision: RL. Funding acquisition, Visualization, Writing original draft, Writing - review & editing: PW.

Competing interests. The contact author has declared that none of the authors has any competing interests.

Financial support. This research was financially supported by the National Natural Science Foundation of China (32460275, 32060244).

References:

An, H., Tang, Z. S., Keesstra, S., and Shangguan, Z. P.: Impact of desertification on soil and plant nutrient stoichiometry in a desert grassland, Sci Rep-Uk, 9, 9422, http://doi.org/10.1038/s41598-019-45927-0, 2019.

Babur, E., Dindaroğlu, T., Riaz, M., and Uslu, O. S.: Seasonal Variations in Litter Layers' Characteristics Control Microbial Respiration and Microbial Carbon Utilization Under Mature Pine, Cedar, and Beech Forest Stands in the Eastern Mediterranean Karstic Ecosystems, Microb. Ecol., 84, 153-167, http://doi.org/10.1007/s00248-021-01842-4, 2022.

Bi, M. F., Zhang, S. P., Xu, Q. X., Hou, S. Z., Han, M. W., and Yu, X. R.: Coupling and synergistic relationships between soil aggregate stability and nutrient stoichiometric characteristics under different microtopographies on karst rocky desertification slopes, Catena, 243, 108142, http://doi.org/10.1016/j.catena.2024.108142, 2024.

Campo, J.: Shift from ecosystem P to N limitation at precipitation gradient in tropical dry forests at Yucatan, Mexico, Environ Res Lett, 11, 95006, http://doi.org/10.1088/1748-9326/11/9/095006, 2016.

Chen, Y., Li, Y. Q., Duan, Y. L., Wang, L. L., Wang, X. Y., Yao, C. P., Chen, Y. P., Cao, W. J., and Niu, Y. Y.: Patterns and driving factors of soil ecological stoichiometry in typical ecologically fragile areas of China, Catena, 219, 106628, http://doi.org/10.1016/j.catena.2022.106628, 2022.

Chen, Z. X., Xu, X., Wen, Y. L., Cheng, M., and Wang, X.: The critical role of soil ecological stoichiometric ratios: How does reforestation improve soil nitrogen and phosphorus availability? Plants, 13, 2320, http://doi.org/10.3390/plants13162320, 2024.

Dindaroglu, T., Babur, E., Battaglia, M., Seleiman, M., Uslu, O. S., and Roy, R.: Impact of Depression Areas and Land-Use Change in the Soil Organic Carbon and Total Nitrogen contents in a Semi-Arid Karst Ecosystem, Cerne, 27, 102980, http://doi.org/10.1590/01047760202127012980, 2021.

Dou, L., Zhang, W., Qin, M. E., Liang, Y. M., and Pan, F. J.: Seasonal variation of ecological stoichiometriccharacteristics of C,N and P in fine roots fromkarst forest and its influencing factors, Guihaia, 44, 452-464, http://doi.org/10.11931/guihaia.gxzw202210018, 2024.

Feng, W. L., Yang, J. L., Xu, L. G., and Zhang, G. L.: The spatial variations and driving factors of C, N, P stoichiometric characteristics of plant and soil in the terrestrial ecosystem, Sci. Total Environ., 951, 175543, http://doi.org/10.1016/j.scitotenv.2024.175543, 2024.

Han, J. J., Duan, X., and Zhao, Y. Y.: Spatial and temporal variability of soil moisture on slope land of different vegetation of dry-hot valley in Jinsha River, Arid Land Geography, 42, 121-129, http://doi.org/10.12118/j.issn.1000-6060.2019.01.14, 2019.

He, X. B., Lin, Y. H., Han, G. M., and Ma, T. W.: Litterfall interception by understorey vegetation delayed litter decomposition in Cinnamomum camphora plantation forest, Plant Soil, 372, 207-219, http://doi.org/10.1007/s11104-

删除[dang]:

References:

An, H., Tang, Z. S., Keesstra, S., and Shangguan, Z. P.: Impact of desertification on soil and plant nutrient stoichiometry in a desert grassland, Sci Rep-Uk, 9, 9422, http://doi.org/10.1038/s41598-019-45927-0, 2019.

Chen, Y., Li, Y. Q., Duan, Y. L., Wang, L. L., Wang, X. Y., Yao, C. P., Chen, Y. P., Cao, W. J., and Niu, Y. Y.: Patterns and driving factors of soil ecological stoichiometry in typical ecologically fragile areas of China, Catena, 219, 106628, http://doi.org/10.1016/j.catena.2022.106628, 2022.

Chen, Z. X., Xu, X., Wen, Y. L., Cheng, M., and Wang, X.: The critical role of soil ecological stoichiometric ratios: How does reforestation improve soil nitrogen and phosphorus availability? Plants, 13, 2320, http://doi.org/10.3390/plants13162320, 2024.

Dindaroglu, T., Babur, E., Battaglia, M., Seleiman, M., Uslu, O. S., and Roy, R.: Impact of Depression Areas and Land-Use Change in the Soil Organic Carbon and Total Nitrogen contents in a Semi-Arid Karst Ecosystem, Cerne, 27, 102980, http://doi.org/10.1590/01047760202127012980, 2021.

Feng, W. L., Yang, J. L., Xu, L. G., and Zhang, G. L.: The spatial variations and driving factors of C, N, P stoichiometric characteristics of plant and soil in the terrestrial ecosystem, Sci. Total Environ., 951, 175543, http://doi.org/10.1016/j.scitotenv.2024.175543, 2024.

Han, J. J., Duan, X., and Zhao, Y. Y.: Spatial and temporal variability of soil moisture on slope land of different vegetation of dry-hot valley in Jinsha River, Arid Land Geography, 42, 121-129, http://doi.org/10.12118/j.issn.1000-6060.2019.01.14, 2019.

Joshi, R. K., and Garkoti, S. C.: Influence of vegetation types on soil physical and chemical properties, microbial biomass and stoichiometry in the central Himalaya, Catena, 222, 106835, http://doi.org/10.1016/j.catena.2022.106835, 2023.

Nagamatsu, D., Hirabuki, Y., and Mochida, Y.: Influence of micro-landforms on forest structure, tree death and recruitment in a Japanese temperate mixed forest, Ecol. Res., 18, 533-547, http://doi.org/10.1046/j.1440-1703.2003.00576.x, 2003.

Peng, X. D., and Dai, Q. H.: Drivers of soil erosion and subsurface loss by soil leakage during karst rocky desertification in SW China, International Soil and Water

013-1734-9, 2013.

Joshi, R. K., and Garkoti, S. C.: Influence of vegetation types on soil physical and chemical properties, microbial biomass and stoichiometry in the central Himalaya, Catena, 222, 106835, http://doi.org/10.1016/j.catena.2022.106835, 2023.

Li, D. J., Wen, L., Zhang, W., Yang, L. Q., Xiao, K. C., Chen, H., and Wang, K. L.: Afforestation effects on soil organic carbon and nitrogen pools modulated by lithology, Forest Ecol. Manag., 400, 85-92, http://doi.org/10.1016/j.foreco.2017.05.050, 2017.

M. Dearden, F., and A. Wardle, D.: The potential for forest canopy litterfall interception by a dense fern understorey, and the consequences for litter decomposition, Oikos, 117, 83-92, http://doi.org/10.1111/j.2007.0030-1299.16136.x, 2008.

Medina, E., Cuevas, E., and Lugo, A.: Substrate Chemistry and Rainfall Regime Regulate Elemental Composition of Tree Leaves in Karst Forests, Forests, 8, 182, http://doi.org/10.3390/f8060182, 2017.

Nagamatsu, D., Hirabuki, Y., and Mochida, Y.: Influence of micro - landforms on forest structure, tree death and recruitment in a Japanese temperate mixed forest, Ecol. Res., 18, 533-547, http://doi.org/10.1046/j.1440-1703.2003.00576.x, 2003.

Pastore, G., Weig, A. R., Vazquez, E., and Spohn, M.: Weathering of calcareous bedrocks is strongly affected by the activity of soil microorganisms, Geoderma, 405, 115408, http://doi.org/10.1016/j.geoderma.2021.115408, 2022.

Perakis, S. S., Sinkhorn, E. R., Catricala, C. E., Bullen, T. D., Fitzpatrick, J. A., Hynicka, J. D., and Cromack, K.: Forest calcium depletion and biotic retention along a soil nitrogen gradient, Ecol. Appl., 23, 1947-1961, http://doi.org/10.1890/12-2204.1, 2013.

Sardans, J., Janssens, I. A., Ciais, P., Obersteiner, M., and Peñuelas, J.: Recent advances and future research in ecological stoichiometry, Perspectives in Plant Ecology, Evolution and Systematics, 50, 125611, http://doi.org/10.1016/j.ppees.2021.125611, 2021.

Silva, M. B., Anjos, L. H. C. D., Pereira, M. G., Schiavo, J. A., Cooper, M., and Cavassani, R. D. S.: Soils in the karst landscape of Bodoquena plateau in cerrado region of Brazil, Catena, 154, 107-117, http://doi.org/10.1016/j.catena.2017.02.022, 2017.

Smirnova, M. A., and Gennadiev, A. N.: Quantitative assessment of pedodiversity and soil erosion within a karst sinkhole in the dry steppe subzone, Eurasian Soil Sci+, 50, 873-884, http://doi.org/10.1134/S1064229317080105, 2017.

Tang, J., Tang, X. X., Qin, Y. M., He, Q. S., Yi, Y., and Ji, Z. L.: Karst rocky desertification progress: Soil calcium as a possible driving force, Sci. Total Environ., 649, 1250-1259, http://doi.org/10.1016/j.scitotenv.2018.08.242, 2019.

Waring, B. G., Sulman, B. N., Reed, S., Smith, A. P., Averill, C., Creamer, C. A., Cusack, D. F., Hall, S. J., Jastrow, J. D., Jilling, A., Kemner, K. M., Kleber, M., Liu, X. J. A., Pett Ridge, J., and Schulz, M.: From pools to flow: The PROMISE framework for new insights on soil carbon cycling in a changing world, Global Change Biol., 26, 6631-6643, http://doi.org/10.1111/gcb.15365, 2020.

Wen, P. Y., and Jin, G. Z.: Effects of topography on species diversity in a typical mixed broadleaved-Korean pine forest, Acta Ecologica Sinica, 39, 945-956, http://doi.org/10.5846/stxb201801110086, 2019.

Wu, P., Zhou, H., Zhao, W. J., Yang, G. N., Cui, Y. C., Hou, Y. J., Tan, C. J., Zhou, T., and Ding, F. J.: Stoichiometric

characteristics and influencing factors of different components of karst forest plants at the microtopography and microhabitat scale in Maolan National Nature Reserve, Guizhou, China, Forests, 16, 317, http://doi.org/10.3390/f16020317, 2025.

Yang, S., Yang, L., Wen, D., Liu, L., Ni, K., Cao, J., Zhu, T., and Müller, C.: Soil calcium constrains nitrogen mineralization and nitrification rates in subtropical karst regions, Soil Biology and Biochemistry, 186, 109176, http://doi.org/10.1016/j.soilbio.2023.109176, 2023.

Yang, Y. C., and Da, L. J.: A brief review of studies on differentiation of vegetation pattern along a topographic gradient in hilly regions, J. Plant Ecol, 30, 504-513, 2006.

Yu, H. Y., Zha, T. G., Zhang, X. X., Nie, L. S., Ma, L. M., and Pan, Y. W.: Spatial distribution of soil organic carbon may be predominantly regulated by topography in a small revegetated watershed, Catena, 188, 104459, http://doi.org/10.1016/j.catena.2020.104459, 2020.

Zhang, C., Zeng, F. P., Zeng, Z. X., Du, H., Zhang, L. J., Su, L., Lu, M. Z., and Zhang, H.: Carbon, Nitrogen and Phosphorus stoichiometry and its influencing factors in karst primary forest, Forests, 13, 1990, http://doi.org/10.3390/f13121990, 2022.

Zhang, Q. P., Fang, R. Y., Deng, C. Y., Zhao, H. J., Shen, M. H., and Wang, Q.: Slope aspect effects on plant community characteristics and soil properties of alpine meadows on Eastern Qinghai-Tibetan plateau, Ecol. Indic., 143, 109400, http://doi.org/10.1016/j.ecolind.2022.109400, 2022.

Zhang, Y. L., Liu, M., Li, H., Yang, J. H., Zhao, X. Y., Qu, J. H., Li, L. J., Bai, Y. L., Yan, D., and Hou, G. N.: Spatial distribution characteristics of soil C:N:P:K eco-stoichiometry of farmland and grassland in the agro-pastoral ecotone in Inner Mongolia, China, Agronomy, 14, 346, http://doi.org/10.3390/agronomy14020346, 2024.

Zhou, T., Cui, Y. C., Ye, Y. Y., Zhao, W. J., Hou, Y. J., Wu, P., and Ding, F.: Leaf functional traits of typical karst forest plants under different niches, Journal of Central South University of Forestry & Technology, 42, 129-140, http://doi.org/10.14067/j.cnki.1673-923x.2022.10.015, 2022.